

and passive feedback [19, 20, 28, 57] that enhance their experience and even enhance the interactivity of the virtual environment. Leveraging the affordances of physical objects could improve user experience and task performance in VR applications [10, 11, 26, 28]. Therefore, some works synthesize virtual scenes based on physical environments [9, 56, 59, 65]. However, these works usually adopt 3D models that are consistent with physical objects [56] (e.g., virtual tables for physical tables), reducing the diversity of virtual scenes. Alternatively, these works may only consider walking areas [9, 59, 65] while neglecting other interactions between users and environments.

In the context of situated scene synthesis, the main goal is to synthesize interactive scenes based on their situated physical environments, considering the affordance of the physical objects. When the user is immersed in the virtual scene, they can also perceive and utilize the affordance of physical objects, which guarantees a highly immersive experience for users. At the same time, it is also necessary to synthesize the virtual scenes that can satisfy users' demands. Generally, users can be immersed in any virtual scene they want if the synthesized scenes are unlimited, so understanding the user's demand is important for meeting personalized requirements. Due to the uncertainty of physical environments and the various personalized needs of users, a well-situated scene synthesis solution should not only exploit the physical objects as building blocks for better physical-virtual consistency but also understand human users' demands via efficient interactions, such as natural language [39, 58].

Therefore, we propose a scene agent, which leverages the large language model's ability of information extraction [33] and its prior knowledge related to scenes [16], that can observe both user demands and the situated physical environments to synthesize virtual scenes with interactivity, as shown in figure 1. For each physical object, the scene agent infers the corresponding virtual object by considering two aspects. One is the affordance similarity between physical objects and virtual objects. Another is the style similarity (including place, season, and object) between user demands and virtual objects. Afterward, according to the physical information, the scene agent synthesizes scenes by translating, rotating, and scaling virtual objects. The synthesized scene can not only maintain the same affordances of physical objects but also maintain the scene style that the user wants.

To the best of our knowledge, this is the first work that synthesizes arbitrary virtual scenes with physical interactivity considering both the physical environment and the user's demand. Overall, our contributions are threefold:

- (1) We propose a language model-based 3D scene synthesis method to extract information of the physical environment, virtual objects, and the user input text, generating their semantic relations for building the interactive agent system.
- (2) We develop a scene agent based on the above method to perceive the physical affordance and user demand, which can synthesize interactive virtual scenes for handling physical constraints and satisfying the user's personalized demands.
- (3) We conduct comparison studies between our method and three baselines, followed by a perceptual study, to demonstrate that the proposed scene agent could synthesize better scenes with affordance maintenance and style maintenance.

2 RELATED WORK

2.1 3D Scene synthesis

Generative models have contributed to the synthesis of outdoor 3D scenes [63]. However, these generated scenes do not support human-object interaction. Researchers synthesize indoor 3D scenes by selecting objects from object datasets and generating layouts based on procedural modeling with grammars [34, 47, 50], graph [35, 38, 61, 68], auto-regressive neural networks [52], transformer [46], and diffusion models [15]. Some methods consider the interaction between humans and environments, such as human motions [51] with human-object contact [66] and poses [67]. Affordance could serve as a bridge to characterize the human-object relations [51]. The aforementioned human-centric scene synthesis methods all took advantage of the object affordance for human-object interaction. However, these works are based on existing human interaction actions. In this work, we will synthesize virtual scenes considering object affordances without human action priors.

2.2 Language-driven 3D Scene synthesis

Language, as an important medium for human-computer interaction, has been used for 3D scene synthesis. RoomDreamer [58] aligned the geometry and texture to the input scene structure and prompt simultaneously. GAUDI [2] was a generative model that enabled both unconditional and conditional synthesis including image, text, category, etc. SceneDreamer [8] synthesized unbounded in-the-wild 3D scenes from 2D images based on the GAN network. CTRL-ROOM [15] controlled the scene synthesis with a diffusion model, enabling the change of scenes. However, those synthesized scenes cannot support immersive interaction in VR. PiGraphs [54] synthesized human pose priors-based scenes that only included human action-related objects mentioned in the language specifications. Chang *et al.* [4–7] and Ma *et al.* [39] parsed the input text into a knowledge tree or graph for synthesis, where the initial scene could be changed by language. These methods aim at indoor scene synthesis, and the input texts need explicit instructions and can only directly specify virtual objects in the database. In this work, we plan to synthesize both indoor and outdoor virtual scenes without explicit instructions.

2.3 Situation-aware scene synthesis

Some works synthesize scenes based on the user-situated physical world. Human-in-loop paradigm-based methods require users to manually place virtual objects in the positions of corresponding physical objects [14, 29]. Other methods adopt the auto-generation paradigm. DreamWalker [65] detected walkable paths and obstacles. The paths are mapped as resembling paths in the virtual scene and the obstacles as default virtual objects. VRoamer [9] and Sra *et al.* [59, 60] extracted walkable areas and physical obstacles according to the scanned physical environment. VRoamer generated corridors and doors for walkable areas while bricks or spikes for obstacles. Sra *et al.* [59, 60] generated boundary elements in the boundary of the walkable areas, where several special objects (e.g. chairs) were mapped as virtual counterparts to leverage the affordance of the physical objects.

Those methods only consider the walkable areas and several special objects, leading to a lack of interactivity in the synthesized 3D scene. Shapira [55] proposed a method that first placed specialized 3D object models in the scene and then optimized their arrangement based on planar areas without considering the interactivity. Our goal is to generate arbitrary scenes which have the same interactivity as the physical world.

3 PRELIMINARY

In this section, we introduce the concepts and symbols adopted.

Scene presentation. A physical environment \mathcal{S}_{phy} including all N physical object information $\{o_n^{phy}\}_{n=1}^N \in \mathcal{O}^{phy}$, where each tuple o_n^{phy} denotes the information of a physical object. A synthesized virtual scene \mathcal{S}_{vir} including a basic scene background b_i^{vir} and all M virtual object information $\{o_m^{vir}\}_{m=1}^M \in \mathcal{O}^{vir}$, where each tuple o_m^{vir} denotes the information of a virtual object. $\mathcal{B} = \{b_h^{vir}\}_{h=1}^H$ denotes all H basic scenes. For a physical object o_i^{phy} or a virtual object o_i^{vir} , it contains attribute information $\{c_i, d_i, t_i, r_i, s_i\}$: category c_i , description d_i (can be empty), bounding box location $t_i = (tx_i, ty_i, tz_i) \in \mathbb{R}^3$, bounding box rotation $r_i = (rw_i, rx_i, ry_i, rz_i) \in \mathbb{R}^4$, and bounding box size $s_i = (sx_i, sy_i, sz_i) \in \mathbb{R}^3$.

Affordance. Affordance was first introduced by psychologist Gibson [18], which represents the action possibilities of an object that are perceivable by an actor [25]. $\mathcal{A} = \{a_k\}_{k=1}^K$ is a tuple of K kind of affordances of an object, where each tuple a_k denotes one kind of affordance. Based on previous works [25, 37], we consider ten different affordances for the objects, including *walkable*, *supportable*, *sitable*, *drinkable*, *eatable*, *graspable*, *breakable*, *dangerous*, *moveable*, *obstructive*.

Virtual place type Theoretically, the types of virtual places can be unlimited. We ask GPT-4 [45] to summarize P virtual place types that people want to go to. We find that when $P > 20$, the types are repeated. Therefore, we select 20 types: *Library*, *Conservatory*, *Spa*, *Lounge*, *Observatory*, *Suite*, *Monastery*, *Studio*, *Bookstore*, *Aquarium*, *Beach*, *Forest*, *Garden*, *Vineyard*, *Yacht*, *Rooftop*, *Treehouse*, *Reef*, *Peak*, *Rainforest*. $\mathcal{E} = \{e_p\}_{p=1}^P$ denotes the tuple of P kinds of virtual places, where e_p denotes the p -th virtual place.

Season Some objects have obvious seasonality, such as a bench covered by snow. We consider the probability that each object can appear in each reason including *spring*, *summer*, *autumn*, *winter*. $\mathcal{T} = \{t_j\}_{j=1}^J$ denotes the tuple of J kinds of seasons, where t_j denotes the j -th season.

User demand Users could express what kind of scene they want to go by a sentence u . Speech is also compatible as it can be converted to texts by speech-to-text techniques. In this paper, we extract **season** t^{user} , **place** type e^{user} , and possible **objects** information from user demand. $\mathcal{O}^{user} = \{o_q^{user}\}_{q=1}^Q$ denotes a tuple of Q kinds of objects mentioned. o_q^{user} only includes the category c .

4 SYNTHESIS METHOD

Our proposed scene agent synthesizes scenes by observing the situated physical environment and the user's demand. The physical

environment information could be obtained via volumetric instance-aware semantics mapping methods from RGB-D information[21, 24]. Our goal is to synthesize user-expected virtual scenes. These scenes maintain the affordances of the physical environment and maintain the style that the user demands. Formally, guided by a physical environment \mathcal{S}_{phy} and a user demand u , the proposed scene agent synthesizes scenes $\mathcal{S}_{vir} \sim \mathcal{P}(\mathcal{S}_{vir} | \mathcal{S}_{phy}, u)$.

Synthesizing a virtual scene with one sentence is a hefty task. Therefore, apart from plain text from the user, we also consider information about the physical environment and virtual objects to solve this problem. The first step is to understand the user's demand. At the same time, we infer the affordance of the situated physical environment. In addition, we infer the features of all virtual objects. Finally, we synthesize the whole virtual scene based on all the results of the first three steps. The whole scene synthesis pipeline is shown in figure 2 and the algorithm is outlined in Algorithm 1.

Algorithm 1 In situ scene synthesis

Input: u : user's input; \mathcal{A} : all affordances; \mathcal{E} : all virtual places; \mathcal{T} : all seasons; \mathcal{O}^{vir} : all virtual objects, $o_m^{vir} \in \mathcal{O}^{vir}$; \mathcal{O}^{phy} : all physical objects, $o_n^{phy} \in \mathcal{O}^{phy}$; $E_{user}(e^{user}, t^{user}, \mathcal{O}^{user} | u)$: text extractor; $L(\cdot, \cdot)$: language similarity; $A(V_{\mathcal{A}} | \mathcal{A}, \mathcal{O})$: affordance predictor; $E(V_{\mathcal{E}} | \mathcal{O})$: place predictor; $T(V_{\mathcal{T}} | \mathcal{O})$: season predictor.

Output: \mathcal{S}_{vir} : the synthesized virtual scene corresponding with the physical environment \mathcal{S}_{phy} .

```

/* User demand inference.*/
1:  $\{e^{user}, t^{user}, \mathcal{O}^{user}\} \sim E_{user}(\cdot | u)$ 
2:  $V_{\mathcal{B}^{user}} \leftarrow L(e^{user}, \mathcal{B}), V_{\mathcal{B}^{user}} \in \mathbb{R}^H$ 
3:  $V_{\mathcal{E}^{user}} \leftarrow L(e^{user}, \mathcal{E}), V_{\mathcal{E}^{user}} \in \mathbb{R}^P$ 
4:  $V_{\mathcal{T}^{user}} \leftarrow L(t^{user}, \mathcal{T}), V_{\mathcal{T}^{user}} \in \mathbb{R}^J$ 
5: for  $q = 1 : Q$  do
6:    $V_{o_q^{user}} \leftarrow L(o_q^{user}, \mathcal{O}^{vir}), o_q^{user} \in \mathcal{O}^{user}, V_{o_q^{user}} \in \mathbb{R}^M$ 
7: end for
8:  $V_{\mathcal{O}^{user}} = [V_{o_1^{user}}, V_{o_1^{user}}, \dots, V_{o_q^{user}}], V_{\mathcal{O}^{user}} \in \mathbb{R}^{Q \times M}$ 
9:  $V_{\mathcal{O}^{user}} = \max_i V_{\mathcal{O}^{user}}[i, j], V_{\mathcal{O}^{user}} \in \mathbb{R}^M$ 
/* Physical affordance inference.*/
10: for  $n = 1 : N$  do
11:    $V_{\mathcal{A}_n^{phy}} \sim A(\cdot | \mathcal{A}, c_n, s_n), \{c_n, s_n\} \in o_n^{phy}, V_{\mathcal{A}_n^{phy}} \in \mathbb{R}^K$ 
12: end for
/* Virtual object-based inference.*/
13: for  $m = 1 : M$  do
14:    $V_{\mathcal{A}_m^{vir}} \sim A(\cdot | \mathcal{A}, c_m, s_m), \{c_m, s_m\} \in o_m^{vir}, V_{\mathcal{A}_m^{vir}} \in \mathbb{R}^K$ 
15:    $V_{\mathcal{E}_m^{vir}} \sim E(\cdot | \mathcal{E}, c_m, d_m), \{c_m, d_m\} \in o_m^{vir}, V_{\mathcal{E}_m^{vir}} \in \mathbb{R}^P$ 
16:    $V_{\mathcal{T}_m^{vir}} \sim T(\cdot | \mathcal{T}, c_m, d_m), \{c_m, d_m\} \in o_m^{vir}, V_{\mathcal{T}_m^{vir}} \in \mathbb{R}^J$ 
17: end for
/* Whole scene synthesis.*/
18:  $b_i^{vir} \leftarrow \arg \max V_{\mathcal{B}^{user}}$ 
19: for  $n = 1 : N$  do
20:    $o_n^{vir} \leftarrow \arg \max_{o_m^{vir} \in \mathcal{O}^{vir}} (C(V_{\mathcal{A}_n^{phy}}, V_{\mathcal{A}_m^{vir}}) * C(V_{\mathcal{E}^{user}}, V_{\mathcal{E}_m^{vir}}) * C(V_{\mathcal{T}^{user}}, V_{\mathcal{T}_m^{vir}}) * S(o_n^{phy}, o_m^{vir}) * (V_{\mathcal{O}^{user}}[m]))$ 
21:    $\{t_n, r_n, s_n\}$  of  $o_n^{vir} \leftarrow IoU(o_n^{vir} | o_n^{phy})$ 
22: end for
23:  $\mathcal{S}_{vir} \leftarrow \text{Load } b_i^{vir}$  and all  $\{o_n^{vir}\}_{n=1}^N$ 

```

233
234
235
236
237
238
239
240
241
242
243
244
245
246
247
248
249
250
251
252
253
254
255
256
257
258
259
260
261
262
263
264
265
266
267
268
269
270
271
272
273
274
275
276
277
278
279
280
281
282
283
284
285
286
287
288
289
290

291
292
293
294
295
296
297
298
299
300
301
302
303
304
305
306
307
308
309
310
311
312
313
314
315
316
317
318
319
320
321
322
323
324
325
326
327
328
329
330
331
332
333
334
335
336
337
338
339
340
341
342
343
344
345
346
347
348

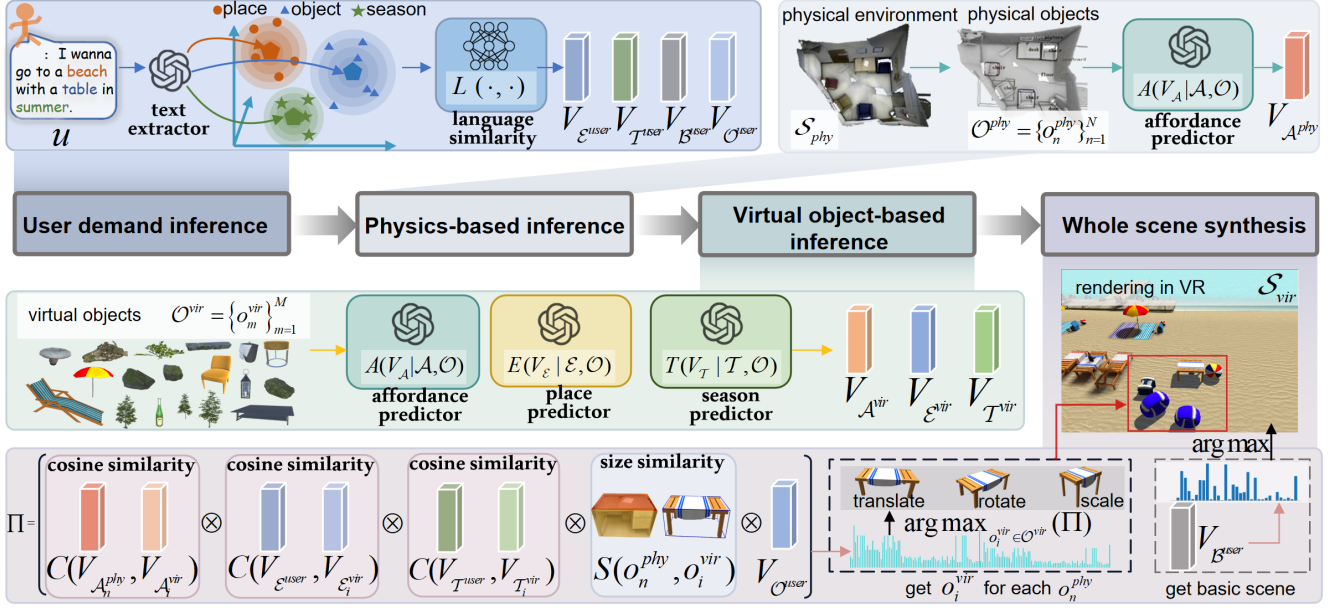


Figure 2: The synthesis algorithm. First, the LLM extracts the place, season, and objects mentioned by the user, which are used to predict the similarity with all places, seasons, and virtual objects via a language similarity module. Moreover, the affordance confidence of each physical object as well as the attribute likelihoods of virtual objects are predicted by the LLM. Next, a cosine similarity module is used to calculate the three similarities: the affordance similarity between each physical object and all virtual objects; the place and season similarities between the virtual objects and the user demand. A size similarity module calculates the size similarity between each physical object and all virtual objects. Finally, the corresponding virtual objects with the highest likelihood for each physical object and the basic scene with the highest likelihood are used for scene synthesis. \otimes means the element-wise multiplication of the vectors of the likelihoods.

4.1 User demand inference

We propose a user text extractor $E_{user}(e^{user}, t^{user}, O^{user}|u)$ based on a large language model (LLM) model which infer the **place** e^{user} , **season** t^{user} , and possible **objects** information O^{user} according to the prompt with the user demand u . e^{user} , t^{user} and O^{user} can be empty. More details about $E_{user}(e^{user}, t^{user}, O^{user}|u)$ can be found in the Appendix.

We adopt the similarity predictor $L(\cdot, \cdot)$ [17] to infer: the scene background similarity $V_{B^{user}} \in \mathbb{R}^H$ between user mentioned place e^{user} and each basic scene b_i^{vir} in \mathcal{B} by $L(e^{user}, \mathcal{B})$; the similarity $V_{E^{user}} \in \mathbb{R}^P$ between user mentioned place e^{user} and each place e_k in \mathcal{E} by $L(e^{user}, \mathcal{E})$; the similarity $V_{T^{user}} \in \mathbb{R}^J$ between user mentioned season t^{user} and each season t_k in \mathcal{T} by $L(t^{user}, \mathcal{T})$; the similarity $V_{O^{user}} \in \mathbb{R}^M$ between all virtual objects O^{vir} and user mentioned objects O^{user} . $V_{O^{user}}$ represents the maximum value of similarity between each virtual object and all objects mentioned by the user. $V_{O^{user}} = \max_i V_{O^{user}}[i, j]$ and $V_{O^{user}} = [V_{O_1^{user}}, V_{O_2^{user}}, \dots, V_{O_q^{user}}]$, $V_{O^{user}} \in \mathbb{R}^{Q \times M}$ and $V_{O^{user}}$ is the similarity matrix of all virtual objects and all objects mentioned in user text u . Specially, if e^{user} , t^{user} or O^{user} is empty, all values of corresponding similarity in $V_{B^{user}}$, $V_{E^{user}}$, $V_{T^{user}}$ or $V_{O^{user}}$ are 1.

4.2 Physics-based inference

For synthesizing scenes where users could take advantage of physical objects' affordance, the affordance of the virtual object should

be aligned with that of the corresponding physical object. Therefore, we propose an affordance LLM-based predictor $A(V_{\mathcal{A}}|\mathcal{A}, \mathcal{O})$ to infer the confidence of each affordance of an object. For the n -th physical object, the affordance confidence $V_{\mathcal{A}_n^{phy}}$ can be got by

$A(\cdot|\mathcal{A}, c_n, s_n), \{c_n, s_n\} \in o_n^{phy}$ according to the prompt with the category c_n and size s_n of the n -th physical object and the affordance list \mathcal{A} . All confidences are represented by a one-dimensional vector. More details about $A(V_{\mathcal{A}}|\mathcal{A}, \mathcal{O})$ can be found in the Appendix.

4.3 Virtual object-based inference

We use the affordance predictor $A(V_{\mathcal{A}}|\mathcal{A}, \mathcal{O})$ to infer the confidence of each affordance of a virtual object. For the m -th virtual object, the affordance confidence $V_{\mathcal{A}_m^{vir}}$ can be got by $A(\cdot|\mathcal{A}, c_m, s_m), \{c_m, s_m\} \in o_m^{vir}$ according to the prompt with its category c_m , its size s_m and the affordance list \mathcal{A} . Additionally, we propose a place predictor $E(V_{\mathcal{E}}|\mathcal{E}, \mathcal{O})$ based on the LLM to infer the likelihood of a virtual object appearing in each virtual place. For the m -th virtual object, its likelihood of appearing in each place $E(V_{\mathcal{E}}|\mathcal{E}, \mathcal{O})$ can be got by $E(\cdot|\mathcal{E}, c_m, s_m, d_m), \{c_m, d_m\} \in o_m^{vir}$ according to the prompt with its category c_m and description d_m . Moreover, we propose a season predictor $T(V_{\mathcal{T}}|\mathcal{T}, \mathcal{O})$ based on the LLM to infer the likelihood of a virtual object appearing in each season. For m -th virtual object, the likelihood of it appearing in each season $V_{T_m^{vir}}$ can be got by $T(\cdot|\mathcal{T}, c_m, s_m), \{c_m, s_m\} \in o_m^{vir}$ according to the prompt with its

category c_m and description d_m . Similarities, confidences, and likelihoods are represented by one-dimensional vectors. More details can be found in the Appendix.

4.4 Scene synthesis

As shown in Algorithm 1, after getting the results of Section 4.1, 4.2 and 4.3, the whole virtual scene can be synthesized. First, we get the basic scene b_i^{vir} corresponding to the maximum value in the basic scene likelihood $V_{\mathcal{B}_{user}}$. We then get the corresponding virtual object o_n^{vir} for each physical object through the maximum value considering two aspects. One is the affordance and size similarities between virtual objects and physical objects. Another is the place, season, and object similarities between virtual objects and the user demand. We propose a module $C(V_i, V_j)$ to calculate the cosine similarity of two vectors and a module $S(o_i, o_j)$ to calculate the size similarity of virtual objects and physical objects. More details about the $S(o_i, o_j)$ can be found in the Appendix. Additionally, we propose an adjusted module $IoU(o^{vir}|o^{phy})$ to get the position, rotation, and size $\{t_n, r_n, s_n\}$ of each virtual object corresponding to the physical object. $IoU(o^{vir}|o^{phy})$ minimizes the value of 3D Intersection over Union (IoU) between the virtual object o_n^{vir} and the physical object o_n^{phy} by adjusting the position, rotation, and size of the virtual object. Finally, we load the selected basic scene b_i^{vir} and all selected virtual objects $\{o_n^{vir}\}_{n=1}^N$ to get the synthesized scene S_{vir} . More details can be found in the Appendix.

5 EXPERIMENT SETUP

5.1 Dataset and Implementation Details

To evaluate the synthesis performance of the proposed method, we use 12 indoor scenes from [13] and 18 scenes from [27] as the physical room input. For each physical room, 12 sentences of user demand are used for scene synthesis. In total, $(12 + 18) * 12 = 360$ synthesized scenes are used for evaluation in the experiments. In addition, a total of 350 virtual objects from three packages in the unity asset store [1, 42, 43] are organized for scene synthesis. Figure 3 demonstrates several synthesized scenes.

5.2 Baselines

We compare the proposed method with three typical baselines: **LLM**, **Semantics**, and **VRoamer**-based methods. Similar to Feng’s work [16], the LLM-based method predicts the corresponding virtual object for each physical object using its information as the prompt. Similar to the methods built-in commercial head-mounted displays [41, 49] which deploy the virtual objects with the same category of physical objects, the Semantics-based method predicts the corresponding virtual object for each physical object based on the language similarity between the virtual and physical objects. VRoamer-based method [9] synthesizes the scene by using virtual objects with *obstructive* affordance. In our VRoamer-based baseline, the virtual objects with a 1.0 confidence of *obstructive* affordance are randomly used to synthesize the scene. In addition, LLM-based, Semantics-based, and VRoamer-based without (w/o) size (**LLM w/o size**, **Semantics w/o size**, **VRoamer w/o size**) or with size (**LLM with size**, **Semantics with size**, **VRoamer with size**) constraints

respectively are compared. Figure 4 demonstrates examples synthesized by different methods. Please find more details about the baselines in the Appendix.

Table 1: Results of quantitative comparison on SceneNN dataset.

Methods	KL Div.(↓)	SD (↑)	Sty. Sim.(↑)	3D IoU (↑)	
				w/ scale	w/o scale
LLM w/o size	0.198	0.134	0.550	0.362	0.114
LLM with size	0.748	0.218	0.554	0.705	0.348
Semantics w/o size	0.149	0.319	0.500	0.486	0.173
Semantics with size	0.217	0.361	0.512	0.743	0.356
VRoamer w/o size	0.455	0.134	0.571	0.349	0.109
VRoamer with size	0.327	0.184	0.568	0.660	0.322
Ours	0.027	0.386	0.763	0.858	0.427

Table 2: Results of quantitative comparison on ProcTHOR dataset.

Methods	KL Div. (↓)	SD (↑)	Sty. Sim.(↑)	3D IoU (↑)	
				w/ scale	w/o scale
LLM w/o size	1.057	0.168	0.533	0.208	0.057
LLM with size	0.364	0.311	0.542	0.620	0.302
Semantics w/o size	0.206	0.493	0.513	0.409	0.148
Semantics with size	0.033	0.545	0.521	0.684	0.338
VRoamer w/o size	1.196	0.207	0.578	0.183	0.051
VRoamer with size	0.854	0.246	0.570	0.381	0.180
Ours	0.042	0.618	0.749	0.729	0.368

5.3 Quantitative evaluation

For indoor scene synthesis, Kullback-Leibler (KL) Divergence between the category distribution of predicted and ground truth scenes and the FID scores of specific projection [16, 48, 52] are usually adopted as evaluation metrics. Our approach synthesizes different scenes without ground truth rather than indoor scenes, leading to the above two metrics are not suitable for evaluating our approach. One of our goals is to synthesize scenes with the same affordance as physical environments. Furthermore, our approach is expected to synthesize scenes containing different types of virtual objects as in physical environments. Therefore, we measure the **affordance maintenance** and **scene diversity** of the synthesized scenes. In addition, we measure **style similarity** between the virtual objects in the synthesized scenes and the user demand and the **3D intersection over union (IoU)** between the physical objects and the corresponding virtual objects. Table 1 and Table 2 show the comparison results compared with six baselines on SceneNN dataset [27] and ProcTHOR dataset [13].

5.3.1 Affordance maintenance. We measure the affordance maintenance via KL Divergence between the affordance class distribution of the virtual objects and the affordance class distribution of the physical objects. The results show that the objects in the scene synthesized by our method have more consistent affordances with physical objects than the baselines.

5.3.2 Scene diversity. We measure the scene diversity (SD) via the number of object type distances between the types of objects in synthesized scenes and in physical environments.

$$SD = 1 - \frac{|N_{syn} - N_{phy}|}{N_{phy}} \quad (1)$$

581
582
583
584
585
586
587
588
589
590
591
592
593
594
595
596
597
598
599
600
601
602
603
604
605
606
607
608
609
610
611
612
613
614
615
616
617
618
619
620
621
622
623
624
625
626
627
628
629
630
631
632
633
634
635
636
637
638

639
640
641
642
643
644
645
646
647
648
649
650
651
652
653
654
655
656
657
658
659
660
661
662
663
664
665
666
667
668
669
670
671
672
673
674
675
676
677
678
679
680
681
682
683
684
685
686
687
688
689
690
691
692
693
694
695
696



Figure 3: The examples of the synthesized scenes of our method.

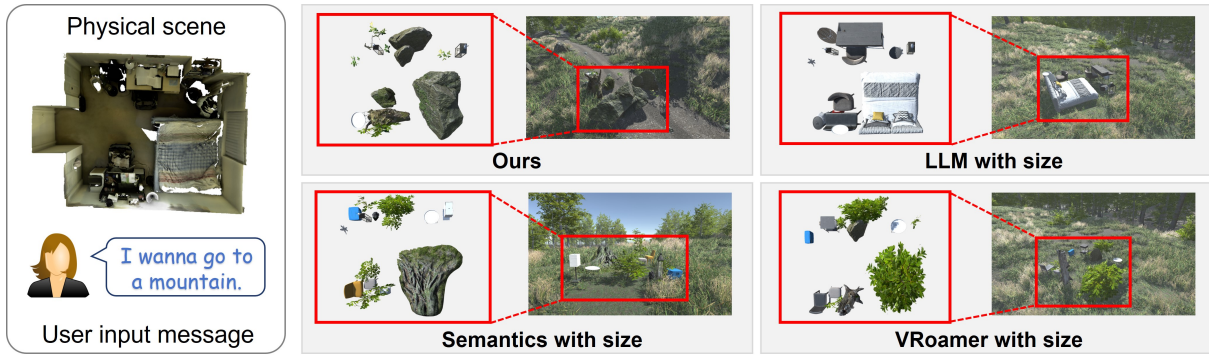


Figure 4: The examples of the synthesized scenes of four methods.

where N_{syn} means the number of types of objects in the synthesized scenes and N_{phy} means that in the physical environments. The bigger value of SD means that synthesized scenes and physical environments have a similar number of object types. The results show that the scenes synthesized by our method have a more similar number of object types to the physical environments compared with the baselines. That means scenes synthesized by our method have a more realistic scene diversity.

5.3.3 Style similarity. We hope the style of virtual objects can meet the user's demands. Therefore, we measure the style similarity (Sty. Sim.) between virtual objects in synthesized scenes and user input.

$$\begin{aligned}
 \text{Sty. Sim.} = & w_1 * \underbrace{\text{Average} \left(\sum_{n=1}^N (V_{Buser} [ind_m] * V_{E_n^{vir}} [ind_m]) \right)}_{\text{scene similarity}} \\
 & + w_2 * \underbrace{\text{Average} \left(\sum_{n=1}^N C(V_{Tuser}, V_{T_{ind_n}^{vir}}) \right)}_{\text{season similarity}} + w_3 * \underbrace{\text{Average} \left(\sum_{n=1}^N V_{O_{ind_n}^{user}} \right)}_{\text{object similarity}}
 \end{aligned} \quad (2)$$

where $w_1 = \frac{1}{3}, w_2 = \frac{1}{3}$, and $w_3 = \frac{1}{3}$ are the weights of the scene similarity, season similarity, and object similarity. ind_m is the index satisfying $V_{Buser} [ind_m] = \arg \max (V_{Buser})$. $V_{Buser} [ind_m]$ means the ind_m -th scene background that best matches user demand. $V_{E_n^{vir}} [ind_m]$ means the likelihood of the n -th object appearing in the ind_m -th scene. ind_n is the index of virtual objects corresponding to the n -th physical objects. $C(V_{Tuser}, V_{T_{ind_n}^{vir}})$ means the similarity between the season likelihood of ind_n -th virtual object matching the seasons mentioned by the users in their demand u . $V_{O_{ind_n}^{user}}$ means the likelihood of the ind_n -th virtual objects matching the objects mentioned in the user demand u . The results show that the scenes synthesized by our method can better maintain the style of the scene that the user demands compared to the baselines.

5.3.4 3D IoU. We measure the 3D intersection over union (IoU) to evaluate the degree of overlap between virtual objects of synthesized scenes and physical objects in physical environments. We compare all methods in two situations: *with (w/) scale* and *without (w/o) scale*. *with (w/) scale* means the virtual objects are scaled according to the size of the physical objects, while *without (w/o) scale* means the virtual objects keep the size of themselves. The scaling

factor is limited to the range from 0.5 to 2 to avoid deforming objects too much. The results show that the scenes synthesized by our method have better 3D IoU.

5.4 Qualitative experiment

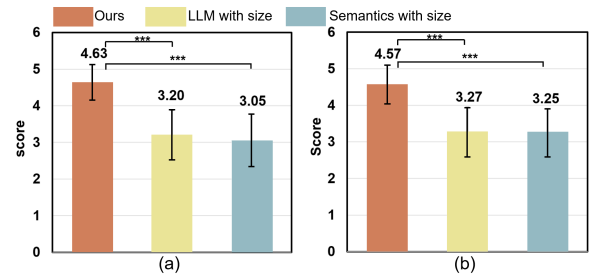


Figure 5: The result of the perceptual study. (a) The scores that the synthesized scene matches the user's description; (b) Affordance and style maintenance of the synthesized scenes. (***) means $p < 0.001$.

We conduct a perceptual study to evaluate the quality of the synthesized scenes as [46]. To this end, we randomly sampled 6 scenes for evaluation. 10 subjects participated in the study. The results of LLM-based without size and semantics-based without size have huge errors. VRoamer-based methods adopt random obstacles to synthesize scenes, which has poor results. Therefore, we compared our methods with **LLM with size** and **Semantics with size** in this perceptual study. Participants filled out scores of the following two questions on a 5-point Likert scale (1 is the least consistent and 5 is the most consistent) for each scene. A total of 60 sets of data are collected. **Q1:** The synthesized scene matches the user's demands. **Q2:** The objects in the synthesized scene maintain affordances to the objects in the physical room and maintain style consistency.

Figure 5 shows the results of the two questions. General repeated measures ANOVA tests and paired T-tests with correction, if needed, are used to analyze the data. There is a significant difference among the three groups (Q1: $F_{2,46.439} = 101.876, p < 0.001$; Q2: $F_{2,39.627} = 100.338, p < 0.001$). The scenes synthesized by our method are significantly better than **LLM with size** (Q1: $t_{59} = 12.672, p < 0.001$, Q2: $t_{59} = 13.105, p < 0.001$) and **Semantics with size** (Q1: $t_{59} = 13.233, p < 0.001$, Q2: $t_{59} = 12.624, p < 0.001$). There is no significant difference between **LLM with size** and **Semantics with size** (Q1: $t_{59} = 1.841, p = 0.071$, Q2: $t_{59} = 0.134, p = 0.894$).

Table 3: Ablation results of SceneNN dataset.

	affordance	place	season	size	object	KL Div. (↓)	SD (↑)	Sty. Sim. (↑)	3D IoU (↑)	
									w/ scale	w/o scale
ours	✓	✓	✓	✓	✓	0.027	0.386	0.763	0.858	0.427
w/o affordance		✓	✓	✓	✓	0.160	0.453	0.803	0.886	0.452
w/o place	✓		✓	✓	✓	0.110	0.369	0.681	0.892	0.453
w/o season	✓	✓		✓	✓	0.025	0.386	0.749	0.864	0.434
w/o size	✓	✓	✓		✓	0.015	0.336	0.695	0.588	0.204
w/o object	✓	✓	✓	✓		0.024	0.387	0.709	0.859	0.432

Table 4: Ablation results of ProcTHOR dataset.

	affordance	place	season	size	object	KL Div. (↓)	SD (↑)	Sty. Sim. (↑)	3D IoU (↑)	
									w/ scale	w/o scale
ours	✓	✓	✓	✓	✓	0.042	0.618	0.749	0.729	0.368
w/o affordance		✓	✓	✓	✓	0.159	0.684	0.778	0.759	0.387
w/o place	✓		✓	✓	✓	0.011	0.526	0.666	0.768	0.409
w/o season	✓	✓		✓	✓	0.041	0.592	0.736	0.738	0.375
w/o size	✓	✓	✓		✓	0.049	0.447	0.807	0.437	0.152
w/o object	✓	✓	✓	✓		0.036	0.618	0.698	0.738	0.376

5.5 Ablation study

We conducted an ablation study to evaluate the effect of each factor. Table 3 and table 4 show the results of the ablation study. The results show that without considering affordances, although the synthesized scenes perform well in terms of scene diversity and style similarity, they do not maintain the affordances of the physical environment well. If place, season, and object are not considered, the performance of style similarity will be even worse. If the size is not considered, the 3D IoU would be relatively poor. In our evaluation, only some user input texts contain season and object information, but it still had an impact on the performance. Given that we aim to synthesize scenes that maintain the physical affordances and style that meets user demands, it is necessary to consider all factors.

6 DISCUSSION

6.1 Unlimited scenes for any physical environment.

Our method enables unlimited scene synthesis according to user demands and physical environments. In particular, if there is no user input, the method still supports the scene synthesis based on the physical environment. The sentence of user demand can be unstructured and arbitrary. It may or may not contain a place, a season, and user-specified objects. In the future, the user demand could be inferred by LLM from a simple sentence, such as *I want to rest*, according to the user's preference. Our method enables the scene synthesis for mixed reality in any physical environment as ubiquitous embodied interfaces, making it possible for future applications, such as virtual offices [23].

6.2 LLM-based prediction

Our method demonstrates a possibility for scene synthesis using the LLM for mixed reality that can be extended in the future. Since our scene agent predicts object properties, including affordances, location, and season, based on the LLM, the results are affected by the inference of the LLM. In the future, more accurate models can improve the performance of our method. In addition, the prompt in our method is based on text only. In the future, the multimodal prompt including images (e.g., images of the virtual objects) could improve the prediction accuracy.

6.3 Diversity of objects

We collect a total of 350 virtual objects in the experiments. A virtual object dataset with a large scale helps synthesize scenes with more styles, to better meet user demands. It can also improve the 3D IoU and the object affordance similarity between synthesized scenes and physical environments. In addition, the virtual objects are retrieved from the dataset in our method, which can also be generated by the example-based [36, 62] or text-based generation methods [44, 64] in the future.

6.4 Virtual objects for physical walls

Our proposed method synthesizes scenes with virtual objects. Although our method can add virtual obstacle objects for physical walls when synthesizing scenes, we found that this is not very reasonable because the user will be surrounded by obstacles in the virtual scenes. We hope to develop a virtual scene with a broad view for users when they are situated in a limited space. In the future, the corresponding virtual objects for physical walls (e.g., [59]) need more studies.

7 CONCLUSION

In this paper, we propose a scene agent to synthesize virtual scenes by observing the situated physical environment and demand of users, which maintains the physical affordance and user-mentioned style. The comparison results show that our method could synthesize better scenes compared with the baselines. Through the scene agent, we hope to provide users with a ubiquitous embodied interface, allowing users to access the immersive virtual environment anytime and anywhere, ensuring security while utilizing the affordance of the physical environment. This can be applied to many areas, such as virtual offices, education, and games. In the future, with the advancement of technologies such as large language models and single object generation, as well as the enrichment of virtual object datasets, our method has the potential to synthesize better scenes. Since our method can be extended based on the similarity of each factor, more factors (e.g., user preferences) can be added to synthesize better scenarios.

REFERENCES

- [1] ArchVizPRO. 2017. ArchVizPRO Interior Vol.5. Retrieved December 19, 2023 from <https://assetstore.unity.com/packages/3d/environments/archvizpro-interior-vol-5-93317>
- [2] Miguel Angel Bautista, Pengsheng Guo, Samira Abnar, Walter Talbott, Alexander Toshev, Zhuoyuan Chen, Laurent Dinh, Shuangfei Zhai, Hanlin Goh, Daniel Ulbricht, et al. 2022. Gaudi: A neural architect for immersive 3d scene generation. *Advances in Neural Information Processing Systems* 35 (2022), 25102–25116.
- [3] Verena Biener, Daniel Schneider, Travis Gesslein, Alexander Otte, Bastian Kuth, Per Ola Kristensson, Eyal Ofek, Michel Pahud, and Jens Grubert. 2020. Breaking the screen: Interaction across touchscreen boundaries in virtual reality for mobile knowledge workers. *IEEE transactions on visualization and computer graphics* 26, 12 (2020), 3490–3502.
- [4] Angel Chang, Will Monroe, Manolis Savva, Christopher Potts, and Christopher D Manning. 2015. Text to 3d scene generation with rich lexical grounding. *arXiv preprint arXiv:1505.06289* (2015).
- [5] Angel Chang, Manolis Savva, and Christopher D Manning. 2014. Learning spatial knowledge for text to 3D scene generation. In *Proceedings of the 2014 conference on empirical methods in natural language processing (EMNLP)*. 2028–2038.
- [6] Angel Chang, Manolis Savva, and Christopher D Manning. 2014. Semantic parsing for text to 3d scene generation. In *Proceedings of the ACL 2014 workshop on semantic parsing*. 17–21.
- [7] Angel X Chang, Mihail Eric, Manolis Savva, and Christopher D Manning. 2017. SceneSeer: 3D scene design with natural language. *arXiv preprint arXiv:1703.00050* (2017).
- [8] Zhaoxi Chen, Guangcong Wang, and Ziwei Liu. 2023. Scenedreamer: Unbounded 3d scene generation from 2d image collections. *arXiv preprint arXiv:2302.01330* (2023).
- [9] Lung-Pan Cheng, Eyal Ofek, Christian Holz, and Andrew D Wilson. 2019. Vroomer: generating on-the-fly VR experiences while walking inside large, unknown real-world building environments. In *2019 IEEE Conference on Virtual Reality and 3D User Interfaces (VR)*. IEEE, 359–366.
- [10] Yi Fei Cheng, Christoph Gebhardt, and Christian Holz. 2023. InteractionAdapt: Interaction-driven Workspace Adaptation for Situated Virtual Reality Environments. In *Proceedings of the 36th Annual ACM Symposium on User Interface Software and Technology*. 1–14.
- [11] Yi Fei Cheng, Tiffany Luong, Andreas Rene Fender, Paul Strelly, and Christian Holz. 2022. ComforTable User Interfaces: Surfaces Reduce Input Error, Time, and Exertion for Tabletop and Mid-air User Interfaces. In *2022 IEEE International Symposium on Mixed and Augmented Reality (ISMAR)*. IEEE, 150–159.
- [12] Emily Dao, Andreea Muresan, Kasper Hornbæk, and Jarrod Knibbe. 2021. Bad breakdowns, useful seams, and face slapping: Analysis of vr fails on youtube. In *Proceedings of the 2021 chi conference on human factors in computing systems*. 1–14.
- [13] Matt Deitke, Eli VanderBilt, Alvaro Herrasti, Luca Weihs, Jordi Salvador, Kiana Ehsani, Winsong Han, Eric Kolve, Ali Farhadi, Aniruddha Kembhavi, and Roozbeh Mottaghi. 2022. ProcTHOR: Large-Scale Embodied AI Using Procedural Generation. In *NewIPS*. Outstanding Paper Award.
- [14] Jose Garcia Estrada and Adalberto L Simeone. 2017. Recommender system for physical object substitution in VR. In *2017 IEEE Virtual Reality (VR)*. IEEE, 359–360.
- [15] Chuan Fang, Xiaotao Hu, Kunming Luo, and Ping Tan. 2023. Ctrl-Room: Controllable Text-to-3D Room Meshes Generation with Layout Constraints. *arXiv preprint arXiv:2310.03602* (2023).
- [16] Weixi Feng, Wanrong Zhu, Tsu jui Fu, Varun Jampani, Arjun Akula, Xuehai He, Sugato Basu, Xin Eric Wang, and William Yang Wang. 2023. LayoutGPT: Compositional Visual Planning and Generation with Large Language Models. [arXiv:2305.15393](https://arxiv.org/abs/2305.15393) [cs.CV]
- [17] Tianyu Gao, Xingcheng Yao, and Danqi Chen. 2021. Simcse: Simple contrastive learning of sentence embeddings. *arXiv preprint arXiv:2104.08821* (2021).
- [18] James Jerome Gibson. 1966. The senses considered as perceptual systems. (1966).
- [19] Mac Greenslade, Adrian Clark, and Stephan Lukosch. 2023. Using Everyday Objects as Props for Virtual Objects in First Person Augmented Reality Games: An Elicitation Study. *Proceedings of the ACM on Human-Computer Interaction* 7, CHI PLAY (2023), 856–875.
- [20] Georges Grinstein, Daniel Keim, and Matthew Ward. 2022. Development of a system for interaction with contextualized real objects in Mixed Reality Environments. Master’s Program in Bioengineering in University of Genoa. <https://unire.unige.it/bitstream/handle/123456789/4266/tesi19383401.pdf?sequence=1&isAllowed=y&group=an>
- [21] Margarita Grinvald, Fadri Furrer, Tonci Novkovic, Jen Jen Chung, Cesar Cadena, Roland Siegwart, and Juan Nieto. 2019. Volumetric instance-aware semantic mapping and 3D object discovery. *IEEE Robotics and Automation Letters* 4, 3 (2019), 3037–3044.
- [22] Jens Grubert, Eyal Ofek, Michel Pahud, and Per Ola Kristensson. 2018. The office of the future: Virtual, portable, and global. *IEEE computer graphics and applications* 38, 6 (2018), 125–133.
- [23] Jie Guo, Dongdong Weng, Zhenliang Zhang, Haiyan Jiang, Yue Liu, Yongtian Wang, and Henry Been-Lirn Duh. 2019. Mixed reality office system based on maslow’s hierarchy of needs: Towards the long-term immersion in virtual environments. In *2019 IEEE International Symposium on Mixed and Augmented Reality (ISMAR)*. IEEE, 224–235.
- [24] Muzhi Han, Zeyu Zhang, Ziyuan Jiao, Xu Xie, Yixin Zhu, Song-Chun Zhu, and Hangxin Liu. 2022. Scene reconstruction with functional objects for robot autonomy. *International Journal of Computer Vision* 130, 12 (2022), 2940–2961.
- [25] Mohammed Hassanin, Salman Khan, and Murat Tahtali. 2021. Visual affordance and function understanding: A survey. *ACM Computing Surveys (CSUR)* 54, 3 (2021), 1–35.
- [26] Steven Henderson and Steven Feiner. 2009. Opportunistic tangible user interfaces for augmented reality. *IEEE Transactions on Visualization and Computer Graphics* 16, 1 (2009), 4–16.
- [27] Binh-Son Hua, Quang-Hieu Pham, Duc Thanh Nguyen, Minh-Khoi Tran, Lap-Fai Yu, and Sai-Kit Yeung. 2016. Scenenn: A scene meshes dataset with annotations. In *2016 fourth international conference on 3D vision (3DV)*. Ieee, 92–101.
- [28] Brent Edward Insko. 2001. *Passive haptics significantly enhances virtual environments*. The University of North Carolina at Chapel Hill.
- [29] Ananya Ipsita, Hao Li, Runlin Duan, Yuanzhi Cao, Subramanian Chidambaram, Min Liu, and Karthik Ramani. 2021. VRFromX: from scanned reality to interactive virtual experience with human-in-the-loop. In *Extended Abstracts of the 2021 CHI Conference on Human Factors in Computing Systems*. 1–7.
- [30] Markus Jelonek. 2023. VRtoER: When Virtual Reality leads to Accidents: A Community on Reddit as Lens to Insights about VR Safety. In *Extended Abstracts of the 2023 CHI Conference on Human Factors in Computing Systems*. 1–6.
- [31] Haiyan Jiang, Dongdong Weng, Zhenliang Zhang, Yihua Bao, Yufei Jia, and Mengnan Nie. 2018. Hikeyb: High-efficiency mixed reality system for text entry. In *2018 IEEE International Symposium on Mixed and Augmented Reality Adjunct (ISMAR-Adjunct)*. IEEE, 132–137.
- [32] Chloe J Jordan and Abraham A Palmer. 2020. Virtual meetings: A critical step to address climate change. , eabe5810 pages.
- [33] Katikapalli Subramanyam Kalyan. 2023. A Survey of GPT-3 Family Large Language Models Including ChatGPT and GPT-4. *arXiv preprint arXiv:2310.12321* (2023).
- [34] Amlan Kar, Aayush Prakash, Ming-Yu Liu, Eric Cameracci, Justin Yuan, Matt Rusiniak, David Acuna, Antonio Torralba, and Sanja Fidler. 2019. Meta-sim: Learning to generate synthetic datasets. In *Proceedings of the IEEE/CVF International Conference on Computer Vision*. 4551–4560.
- [35] Manyi Li, Akshay Gadi Patil, Kai Xu, Siddhartha Chaudhuri, Owais Khan, Ariel Shamir, Changhe Tu, Baoquan Chen, Daniel Cohen-Or, and Hao Zhang. 2019. Grains: Generative recursive autoencoders for indoor scenes. *ACM Transactions on Graphics (TOG)* 38, 2 (2019), 1–16.
- [36] Weiylu Li, Xuelin Chen, Jue Wang, and Baoquan Chen. 2023. Patch-based 3D Natural Scene Generation from a Single Example. In *Proceedings of the IEEE/CVF Conference on Computer Vision and Pattern Recognition*. 16762–16772.
- [37] Timo Luddecke and Florentin Worgotter. 2017. Learning to segment affordances. In *Proceedings of the IEEE International Conference on Computer Vision Workshops*. 769–776.
- [38] Andrew Luo, Zhoutong Zhang, Jiajun Wu, and Joshua B Tenenbaum. 2020. End-to-end optimization of scene layout. In *Proceedings of the IEEE/CVF Conference on Computer Vision and Pattern Recognition*. 3754–3763.
- [39] Rui Ma, Akshay Gadi Patil, Matthew Fisher, Manyi Li, Sören Pirk, Binh-Son Hua, Sai-Kit Yeung, Xin Tong, Leonidas Guibas, and Hao Zhang. 2018. Language-driven synthesis of 3D scenes from scene databases. *ACM Transactions on Graphics (TOG)* 37, 6 (2018), 1–16.
- [40] Mark McGill, Daniel Boland, Roderick Murray-Smith, and Stephen Brewster. 2015. A dose of reality: Overcoming usability challenges in vr head-mounted displays. In *Proceedings of the 33rd annual ACM conference on human factors in computing systems*. 2143–2152.
- [41] Meta. [n. d.]. Meta Quest 3. Retrieved January 11, 2024 from <https://about.fb.com/news/2023/09/meet-meta-quest-3-mixed-reality-headset/>
- [42] Mixall. 2020. Beach - resort. Retrieved December 19, 2023 from <https://assetstore.unity.com/packages/3d/props/beach-resort-127625>
- [43] NatureManufacture. 2023. Forest Environment - Dynamic Nature. Retrieved December 19, 2023 from <https://assetstore.unity.com/packages/3d/vegetation/forest-environment-dynamic-nature-150668>
- [44] Alex Nichol, Heewoo Jun, Prafulla Dhariwal, Pamela Mishkin, and Mark Chen. 2022. Point-e: A system for generating 3d point clouds from complex prompts. *arXiv preprint arXiv:2212.08751* (2022).
- [45] OpenAI. [n. d.]. ChatGPT. <https://openai.com/blog/chatgpt>.
- [46] Wamiq Reyaz Para, Paul Guerrero, Niloy Mitra, and Peter Wonka. 2023. COFS: Controllable furniture layout synthesis. In *ACM SIGGRAPH 2023 Conference Proceedings*. 1–11.
- [47] Yoav IH Parish and Pascal Müller. 2001. Procedural modeling of cities. In *Proceedings of the 28th annual conference on Computer graphics and interactive techniques*. 301–308.

929
930
931
932
933
934
935
936
937
938
939
940
941
942
943
944
945
946
947
948
949
950
951
952
953
954
955
956
957
958
959
960
961
962
963
964
965
966
967
968
969
970
971
972
973
974
975
976
977
978
979
980
981
982
983
984
985
986987
988
989
990
991
992
993
994
995
996
997
998
999
1000
1001
1002
1003
1004
1005
1006
1007
1008
1009
1010
1011
1012
1013
1014
1015
1016
1017
1018
1019
1020
1021
1022
1023
1024
1025
1026
1027
1028
1029
1030
1031
1032
1033
1034
1035
1036
1037
1038
1039
1040
1041
1042
1043
1044

- 1045 [48] Despoina Paschalidou, Amlan Kar, Maria Shugrina, Karsten Kreis, Andreas Geiger,
1046 and Sanja Fidler. 2021. Atiss: Autoregressive transformers for indoor scene
1047 synthesis. *Advances in Neural Information Processing Systems* 34 (2021), 12013–
1048 12026.
- 1049 [49] Pico. [n. d.]. Pico 4. Retrieved January 11, 2024 from [https://www.picoxr.com/
1050 global/products/pico4](https://www.picoxr.com/global/products/pico4)
- 1051 [50] Pulak Purkait, Christopher Zach, and Ian Reid. 2020. Sg-vae: Scene grammar
1052 variational autoencoder to generate new indoor scenes. In *European Conference
1053 on Computer Vision*. Springer, 155–171.
- 1054 [51] Siyuan Qi, Yixin Zhu, Siyuan Huang, Chenfanfu Jiang, and Song-Chun Zhu. 2018.
1055 Human-centric indoor scene synthesis using stochastic grammar. In *Proceedings
1056 of the IEEE Conference on Computer Vision and Pattern Recognition*. 5899–5908.
- 1057 [52] Daniel Ritchie, Kai Wang, and Yu-an Lin. 2019. Fast and flexible indoor scene syn-
1058 thesis via deep convolutional generative models. In *Proceedings of the IEEE/CVF
1059 conference on computer vision and pattern recognition*. 6182–6190.
- 1060 [53] Anastasia Ruvimova, Junhyeok Kim, Thomas Fritz, Mark Hancock, and David C
1061 Shepherd. 2020. "Transport Me Away": Fostering Flow in Open Offices through
1062 Virtual Reality. In *Proceedings of the 2020 CHI conference on human factors in
1063 computing systems*. 1–14.
- 1064 [54] Manolis Savva, Angel X. Chang, Pat Hanrahan, Matthew Fisher, and Matthias
1065 Nießner. 2016. PiGraphs: Learning Interaction Snapshots from Observations.
1066 *ACM Trans. Graph.* 35, 4, Article 139 (jul 2016), 12 pages. [https://doi.org/10.1145/
1067 2897824.2925867](https://doi.org/10.1145/2897824.2925867)
- 1068 [55] Lior Shapira and Daniel Freedman. 2016. Reality skins: Creating immersive and
1069 tactile virtual environments. In *2016 IEEE International Symposium on Mixed and
1070 Augmented Reality (ISMAR)*. IEEE, 115–124.
- 1071 [56] Lior Shapira and Daniel Freedman. 2016. Reality skins: Creating immersive and
1072 tactile virtual environments. In *2016 IEEE International Symposium on Mixed and
1073 Augmented Reality (ISMAR)*. IEEE, 115–124.
- 1074 [57] Adalberto L Simeone, Eduardo Velloso, and Hans Gellersen. 2015. Substitutional
1075 reality: Using the physical environment to design virtual reality experiences. In
1076 *Proceedings of the 33rd Annual ACM Conference on Human Factors in Computing
1077 Systems*. 3307–3316.
- 1078 [58] Liangchen Song, Liangliang Cao, Hongyu Xu, Kai Kang, Feng Tang, Junsong Yuan,
1079 and Yang Zhao. 2023. RoomDreamer: Text-Driven 3D Indoor Scene Synthesis
1080 with Coherent Geometry and Texture. *arXiv preprint arXiv:2305.11337* (2023).
- 1081 [59] Misha Sra, Sergio Garrido-Jurado, and Pattie Maes. 2017. Oasis: Procedurally
1082 generated social virtual spaces from 3d scanned real spaces. *IEEE transactions on
1083 visualization and computer graphics* 24, 12 (2017), 3174–3187.
- 1084 [60] Misha Sra, Sergio Garrido-Jurado, Chris Schmandt, and Pattie Maes. 2016. Pro-
1085 cedurally generated virtual reality from 3D reconstructed physical space. In
1086 *Proceedings of the 22nd ACM Conference on Virtual Reality Software and Technol-
1087 ogy*. 191–200.
- 1088 [61] Kai Wang, Yu-An Lin, Ben Weissmann, Manolis Savva, Angel X Chang, and
1089 Daniel Ritchie. 2019. Planit: Planning and instantiating indoor scenes with
1090 relation graph and spatial prior networks. *ACM Transactions on Graphics (TOG)*
1091 38, 4 (2019), 1–15.
- 1092 [62] Rundi Wu, Ruoshi Liu, Carl Vondrick, and Changxi Zheng. 2023. Sin3DM:
1093 Learning a Diffusion Model from a Single 3D Textured Shape. *arXiv preprint
1094 arXiv:2305.15399* (2023).
- 1095 [63] Haozhe Xie, Zhaoxi Chen, Fangzhou Hong, and Ziwei Liu. 2023. CityDreamer:
1096 Compositional Generative Model of Unbounded 3D Cities. *arXiv preprint
1097 arXiv:2309.00610* (2023).
- 1098 [64] Jiale Xu, Xintao Wang, Weihao Cheng, Yan-Pei Cao, Ying Shan, Xiaohu Qie,
1099 and Shenghua Gao. 2023. Dream3d: Zero-shot text-to-3d synthesis using 3d
1100 shape prior and text-to-image diffusion models. In *Proceedings of the IEEE/CVF
1101 Conference on Computer Vision and Pattern Recognition*. 20908–20918.
- 1102 [65] Jackie Yang, Christian Holz, Eyal Ofek, and Andrew D Wilson. 2019.
1103 Dreamwalker: Substituting real-world walking experiences with a virtual reality.
1104 In *Proceedings of the 32nd Annual ACM Symposium on User Interface Software and
1105 Technology*. 1093–1107.
- 1106 [66] Sifan Ye, Yixing Wang, Jiaman Li, Dennis Park, C. Karen Liu, Huazhe Xu, and
1107 Jiajun Wu. 2022. Scene Synthesis from Human Motion. In *SIGGRAPH Asia 2022
1108 Conference Papers* (Daegu, Republic of Korea) (SA '22). Association for Computing
1109 Machinery, New York, NY, USA, Article 26, 9 pages. [https://doi.org/10.1145/
1110 3550469.3555426](https://doi.org/10.1145/3550469.3555426)
- 1111 [67] Hongwei Yi, Chun-Hao P Huang, Shashank Tripathi, Lea Hering, Justus Thies,
1112 and Michael J Black. 2023. MIME: Human-Aware 3D Scene Generation. In
1113 *Proceedings of the IEEE/CVF Conference on Computer Vision and Pattern Recognition*.
1114 12965–12976.
- 1115 [68] Yang Zhou, Zachary While, and Evangelos Kalogerakis. 2019. Scenegrphnet:
1116 Neural message passing for 3d indoor scene augmentation. In *Proceedings of the
1117 IEEE/CVF International Conference on Computer Vision*. 7384–7392.
- 1118
1119
1120
1121
1122
1123
1124
1125
1126
1127
1128
1129
1130
1131
1132
1133
1134
1135
1136
1137
1138
1139
1140
1141
1142
1143
1144
1145
1146
1147
1148
1149
1150
1151
1152
1153
1154
1155
1156
1157
1158
1159
1160